

RESEARCH PAPER



## Desmoglein-2 as a prognostic and biomarker in ovarian cancer

Jiho Kim<sup>a,b</sup>, Peter Beidler<sup>a</sup>, Hongjie Wang<sup>a</sup>, Chang Li<sup>a</sup>, Abdullah Quassab<sup>c</sup>, Cari Coles<sup>a</sup>, Charles Drescher<sup>d</sup>, Darrick Carter<sup>b,e</sup>, and André Lieber<sup>a,c</sup>

<sup>a</sup>Division of Medical Genetics, Department of Medicine, University of Washington, Seattle, Washington, USA; <sup>b</sup>R&D Department, PAI Life Sciences Inc, Seattle, Washington, USA; <sup>c</sup>Department of Pathology, University of Washington, Seattle, Washington, USA; <sup>d</sup>Public Health Sciences, Fred Hutchinson Cancer Research Center, Seattle, Washington, USA; <sup>e</sup>R&D Department, Onc Bio, Seattle, Washington, USA

### ABSTRACT

Greater than 80% of all cancer cases are carcinomas, formed by the malignant transformation of epithelial cells. One of the key features of epithelial tumors is the presence of intercellular junctions, which link cells to one another and act as barriers to the penetration of molecules. This study assessed the expression of desmoglein-2, an epithelial junction protein, as a prognostic and diagnostic biomarker for ovarian cancer. Ovarian cancer sections were stained for DSG2 and signal intensity was correlated to cancer type and grade. DSG2 immunohistochemistry signals and mRNA levels were analyzed in chemo-resistant and chemo-sensitive cases. Ovarian cancer patient serum levels of shed DSG2 were correlated to disease-free and overall survival. Primary ovarian cancer cells were used to study DSG2 levels as they changed in response to cisplatin treatment. DSG2 expression was found to be positively correlated with cancer grade. Ovarian cancer patients with high serum levels of shed DSG2 fared significantly worse in both progression-free survival (median survival of 16 months vs. 26 months,  $p = .0023$ ) and general survival (median survival of 37 months vs. undefined,  $p < .0001$ ). A subgroup of primary chemotherapy-resistant cases had stronger DSG2 IHC/Western signals and higher DSG2 mRNA levels. Furthermore, our *in vitro* studies indicate that non-cytotoxic doses of cisplatin can enhance DSG2 expression, which, in turn, can contribute to chemo-resistance. We suggest that DSG2 can be used in stratifying patients, deciding on where to use aggressive treatment strategies, predicting chemoresistance, and as a companion diagnostic for treatments targeting DSG2.

### ARTICLE HISTORY

Received 4 May 2020  
Revised 20 October 2020  
Accepted 21 October 2020

### KEYWORDS

Ovarian cancer; biomarkers; epithelial junctions; prognostic; desmoglein

### Introduction

Although incidence rates of ovarian cancer have been falling over the last few decades, it still ranks as the deadliest of any cancer in the female reproductive tract. An estimated 22,530 new diagnoses and 13,980 deaths will occur in the United States in 2019<sup>1</sup>, representing a significant burden in women's health. When diagnosed, the overall 5-y survival rate in the US is 45%. The main histological types of epithelial ovarian cancer are high-grade serous carcinoma (~70%), clear cell carcinoma (~10%), endometrioid carcinoma (~10%), low-grade-serous carcinoma (<5%), and mucinous carcinoma (<5%). Disease stages are stage 1 (cancer is confined to one or both ovaries), stage 2 (cancer spreads within the pelvic region), stage 3 (cancer spreads to other body parts within the abdomen or retroperitoneal lymph nodes), and stage 4 (cancer spreads beyond the abdomen or directly involves the or spleen).

A persistent problem in solid tumor therapy is the presence of physical barriers, which may act to prevent drug entry and penetration.<sup>2</sup> Epithelial junctions are of particular interest in physical barrier formation, as the structure of a tight junction can exclude entry of molecules as small as 400 Daltons.<sup>3</sup> These junctions are involved in the regulation of ion transport across epithelia, preservation of structural integrity and exclude entry of microbes, or – in the case of malignant tumors –

therapeutics. Epithelial junctions include tight junctions, desmosomes, gap junctions, and adherens junctions. Tight junctions, also called zonula occludens, are often found in locations where the impermeability of soluble molecules is required, such as in the gastro-intestinal or airway tracts.<sup>4</sup> Several pathogens subvert the tight junctions as means of entry, including enteropathogenic *E. coli*, and *Salmonella*.<sup>5</sup> Several types of adenoviruses target multiple receptors involved in the formation of epithelial junctions including the CAR, the coxsackievirus receptor, and DSG2, the adenovirus receptor.<sup>6,7</sup>

DSG2 is a calcium-binding transmembrane glycoprotein belonging to the cadherin protein family. It is a key component of desmosomal junctions responsible for forming cell-to-cell junctions and as an anchor for intermediate filaments.<sup>8</sup> It has been reported that epidermal growth factor receptor (EGFR) activation triggers tyrosine phosphorylation of DSG2 and subsequent modulation of cell–cell interaction, in part through the activation of matrix metalloprotease (MMP) cleavage of DSG2 homodimers between neighboring epithelial cells.<sup>9</sup> This cleavage results in shedding of the extracellular domain of DSG2. In xenograft tumor models, shed DSG2 can be detected in the serum.<sup>10</sup>

DSG2 has been observed to be overexpressed and a predictor of poor prognosis in multiple types of cancer, including skin,<sup>11,12</sup> non-small cell lung cancer,<sup>13</sup> lung

adenocarcinoma,<sup>14,15</sup> hepatocellular carcinoma,<sup>16</sup> and gastric cancer,<sup>17</sup> indicating that tumors can take advantage of DSG2 overexpression as a means of forming tight physical barriers and contributing to resistance against therapeutics.<sup>15,18,19</sup>

This makes DSG2 an appealing target: compromising it in solid tumors would result in enhanced permeation or penetration of therapeutics and immune cells. We have previously explored this option using an engineered form of the adenovirus subtype 3 fiber knob protein (Junction Opener or “JO”), which mediates binding to the DSG2 protein, its cleavage/downregulation, and transient opening of epithelial junctions.<sup>7,10,20–24</sup>

In the context of ovarian cancer, several studies have found preliminary evidence of DSG2 overexpression. A proteome analysis of ovarian cancer ascites found DSG2 upregulated and suggested it as a potential biomarker for ovarian cancer.<sup>25</sup> mRNA profiling using the TCGA data set found that upregulated DSG2 expression correlated with worse high-grade serous ovarian cancer (HGSC) prognosis among platinum-sensitive patients.<sup>26</sup> Chen et al. correlated DSG2 expression and survival of ovarian cancer patients and concluded that DSG2 may be involved in the progression of specific types of ovarian cancer.<sup>27</sup>

Here we specifically investigated DSG2, including shed serum DSG2, as a potential ovarian cancer biomarker. We found a significant correlation of DSG2 overexpression with shorter progression-free survival, overall survival, and chemoresistance. The outcome of this study is also relevant for an upcoming clinical trial, which is focused on the clinical translation of JO in combination with PEGylated liposomal doxorubicin (PLD)/Doxil® for ovarian cancer therapy.<sup>28</sup> In this context, we plan to measure DSG2 levels in patient biopsies and serum and correlate these data with treatment outcomes.

Our study is also relevant for DSG2-targeting oncolytic adenoviruses, including Ad5/3 and Ad3-based vectors<sup>7,29–32</sup> specifically against ovarian cancer expressing high levels of DSG2.

## Results

### *DSG2 is overexpressed in ovarian cancer primary and metastatic tissue*

A series of ovarian cancer tissue slides were stained for DSG2. Ovarian primary cancer tissue of serous, clear cell, and endometrioid origin showed localization of the highest DSG2 expression at the cell-cell junctions, as expected, although a scattered distribution of DSG2 staining was present along the cell membrane (Figure 1(a), S1, and S2). Metastatic tissue showed similar expression patterns toward the periphery of the lesion with relatively more uniform distribution throughout the core of the tumor (Figure 1(b)). Immunofluorescent staining of a xenograft tumor derived from a primary ovarian cancer cell line, ovc316,<sup>33,34</sup> showed abundant levels of DSG2 at the edges of the tissue co-localizing with claudin-7, another key junction protein (Figure 1(c), S3). This indicated that ovarian cancer tissue of primary, metastatic, and cell line origins have predominant membrane-localized DSG2, whereby it is not exclusively trapped in junctions and accessible to potential ligands.

### *DSG2 is differentially expressed by class and grade of ovarian cancer*

To obtain more quantitative data, an ovarian cancer tissue array was stained for DSG2 using identical antibodies to those used for the clinical samples above. The tissue array contained a variety of ovarian cancer tissues ranging in grades from 1 to 3 and classified as mucinous, serous, metastatic, or normal (see Table S1 for patient information). Initial DSG2 staining showed progressive increases in DSG2 staining intensity with higher grades, seen throughout the entire section with concentration near cell-cell junctions (Figure 2(a), S4). Analysis of DSG2 signals using Visiopharm software allowed for a quantification of the ratio of DSG2<sup>+</sup> regions (as defined by a threshold of pixel intensity values) compared to the total area of the tissue section. Using this measure, a comparison of

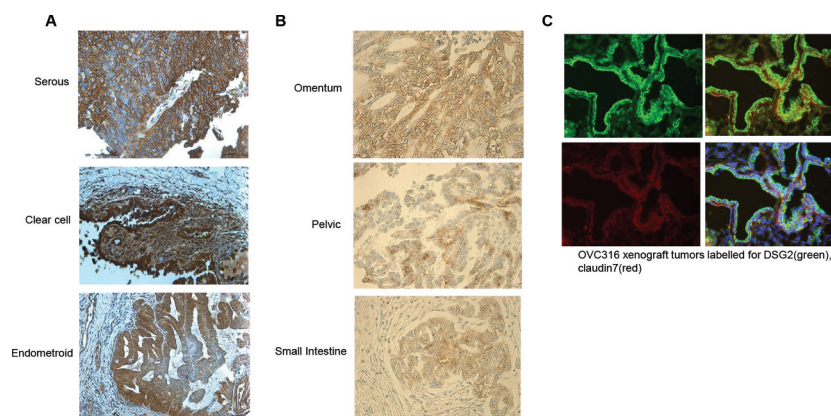


**Figure 1.** DSG2 is differentially expressed in ovarian primary, metastatic tumors and cell lines. **(A)** Representative clinical samples of serous ( $n = 21$ ), clear cell ( $n = 11$ ), and endometrioid tumors ( $n = 10$ ). Paraffin sections were stained for DSG2 (brown) and counterstained with hematoxylin/eosin. **(B)** Representative clinical samples of metastases at the omentum ( $n = 12$ ), pelvis ( $n = 7$ ), and small intestine ( $n = 4$ ) of ovarian origin stained for DSG2 with hematoxylin/eosin counterstain. **(C)** Xenograft tumor derived from injected ovc316 cells, a primary ovarian cancer cell line. Cryosections were stained for DSG2 and claudin 7 with secondary antibodies conjugated to FITC (DSG2-green) or PE (claudin 7-red). Cell nuclei were stained with DAPI (blue).

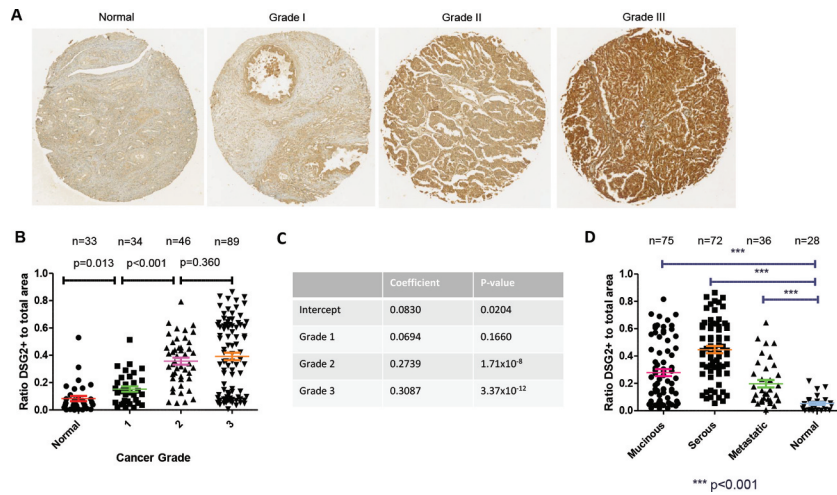


**Figure 2.** DSG2 is differentially expressed in ovarian cancers by grade and pathologic classification (localization). Commercially available ovarian cancer tissue panels were stained for DSG2 and analyzed for staining intensity. **(A)** Representative DSG2 stains of different ovarian cancer tissue classified by grade, from normal to grade 3 (40 $\times$  magnification). **(B)** DSG2 stains of different ovarian tissues classified by grade, from normal tissue (not malignant or benign) to cancerous grades 1–3 (20 $\times$  magnification). DSG2 staining intensity was quantified using Visiopharm software, with analysis parameters outlined in the “Materials and Methods” Section. *P* values represent statistical significance determined with pairwise comparisons using the Student’s *t*-test. Error bars indicate 95% confidence intervals. **(C)** Coefficient and *P* values for linear regression modeling of DSG2+ ratio by grade, using normal grade as a base. Coefficient and *P* value with null hypothesis of coefficient = 0 is shown. **(D)** Numerical comparison of DSG2 signals by histological classification. “mucinous”: mucinous primary tumor; “serous”: serous primary tumor; “Metastases”: metastatic lesion derived from serous ovarian cancer. Error bars indicate 95% confidence intervals.

DSG2<sup>+</sup> ratios between grades found significant differences between normal nonmalignant tissues, grade 1, and grade 2 tissues, and a trend between grades 2 and 3 (Figure 2(b)). A linear regression using the histopathological grading resulted in significant differences associated with grades 2 and 3 when compared to normal tissue (Figure 2(c)). Strikingly, when grade 1 alone was compared to grades 2 + 3 together, mean DSG2+ ratios were 0.199 and 0.451, respectively ( $p < .0001$ ). When analyzed by histological subtype or location (primary vs metastatic), serous ovarian cancer showed the highest DSG2 staining, followed by mucinous and metastatic tissues (Figure 2(d)). All cancerous tissue, including metastatic lesions, showed elevated DSG2 staining in comparison to normal tissue. Thus, DSG2 is increasingly expressed on higher grade ovarian cancers and is differentially expressed in varied presentations of ovarian cancer.

### DSG2 is differentially expressed in chemo-resistant relative vs chemo-sensitive ovarian cancer

Considering the fact that epithelial junctions represent physical barriers to intratumoral penetration of chemotherapeutic drugs, we hypothesized that DSG2 expression and presence in epithelial junctions would correlate with resistance to chemotherapy. We, therefore, focused on ovarian cancer biopsies from patients that were classified as chemo-resistant and chemo-sensitive. Chemo-resistant cases were defined as follows: *i*) progression through or persistence at the completion of primary chemotherapy and *ii*) complete response to primary platinum combination chemotherapy but disease recurrence within 6 months. Chemo-sensitive cases were defined as patients with complete response to primary chemotherapy and a progression-free interval (PFI) of at least 24 months.<sup>35</sup>

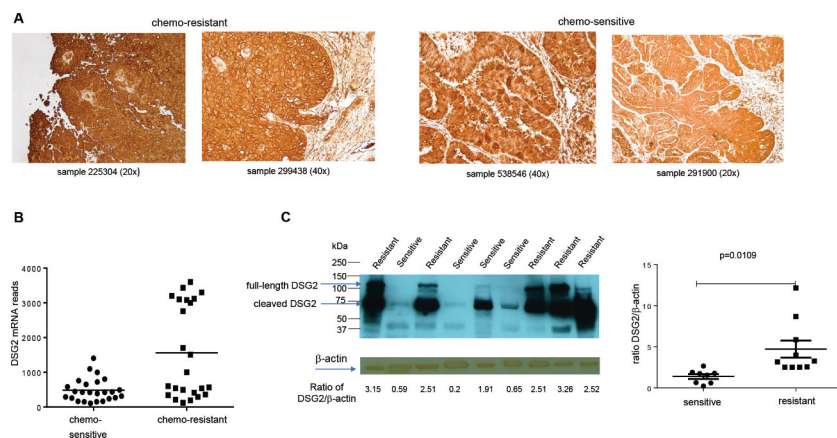


**Figure 3.** DSG2 expression in chemo-resistant and chemo-sensitive tumors. **(A)** Representative tumor sections from patients classified as chemo-resistant or chemo-sensitive were stained for DSG2 (brown). **(B)** DSG2 mRNA levels in cohorts of chemo-sensitive and chemo-resistant ovarian cancer patients ( $n = 49$ ). Shown are DSG2 mRNA reads as detected by RNA-seq. **(C)** DSG2 Western blot of biopsy lysates from chemo-resistant or chemo-sensitive patients. Left panel: A set of representative samples are shown. Right panel: DSG2 Western blot signals normalized to β-actin. Each symbol represents an individual patient.

Staining of DSG2 on chemo-resistant ovarian cancer sections demonstrated stronger DSG2 signals in the cell membranes (Figure 3(a), left panels). In contrast, DSG2 staining was less membrane-localized on chemo-sensitive cases (Figure 3(a) right panels).

In another set of ovarian cancer biopsy samples (25 chemo-resistant and 24 chemo-sensitive cases), we measured DSG2 mRNA by RNA-Seq. Samples from chemo-resistant patients showed significantly higher reads of DSG2 mRNA when compared to chemo-sensitive cases (Figure 3(b)). Interestingly, even within the chemo-resistant DSG2-high population, a clustering of two distinct populations occurred, indicating high DSG2 expression as a partially associated, but not solely responsible factor with chemo-resistance. A similar expression pattern was observed by Western blot analysis of ovarian cancer lysates using DSG2-specific antibodies (Figure 3(c)).

### Serum DSG2 levels are associated with ovarian cancer survival

To further explore the differential DSG2 expression in ovarian cancer patients, we measured shed DSG2 in serum samples of 23 patients with advanced-stage ovarian/fallopian tube cancer<sup>36</sup> (Figure 4 and S5). Blood was drawn after front line surgery. All patients received six cycles of a carboplatin-taxane combination therapy. Twenty patients developed recurrent disease and were used for marker evaluation. Patients were classified as serum DSG2-high (>828 ng/ml) or DSG2-low (<828 ng/ml). The DSG2 threshold reflected the mean DSG2 concentration of the cohort (Fig. S5).

DSG2-high patients had a significantly shorter progression-free survival ( $p = .0096$ ) and overall survival ( $p = .0003$ ) (Figure 4, S5). The average time until progression was markedly different in the groups, with the DSG2-high population averaging a progression-free survival (PFS) of only 16 months vs 26 months in the DSG2-low population. The drastic difference in survival and progression in ovarian cancer patients may highlight the importance of DSG2 in mediating chemoresistance and faster progression and the potential of DSG2 to be used as a prognostic marker to predict patient outcomes.

### DSG2 levels increase in tumor cells treated with chemotherapy

The most probable explanation for the upregulation of DSG2 in cancers is to enforce the epithelial barriers which preclude the entry of chemotherapeutics. This could be a process that is

triggered in cells that were exposed to non-cytotoxic doses of chemotherapeutic drugs, e.g. tumor cells distant to blood vessels.<sup>37,38</sup> To support this hypothesis, we exposed three different ovarian cancer cell lines (OVCAR3, OVCAR5-RFP, and ovc316) to cisplatin for 6 d and analyzed DSG2 (Figure 5). All three cell lines were 100% positive for DSG2 as measured by flow cytometry (Figure 5(a)). In previous studies<sup>33</sup> and additional preliminary studies, we determined that a concentration of 2.5  $\mu$ M cisplatin did not decrease the viability of ovc316 and OVCAR5-RFP by more than 10%. In contrast, this dose killed 95% of OVCAR3 cells by day 6, demonstrating the cytostatic effect of the chemotherapy drug. The latter is also shown by the disappearance of Western blot DSG2 signals at day 6 of cisplatin treatment (Figure 5(b)). On day 6, more full-length and cleaved DSG2 was detected by Western blot in samples treated with cisplatin compared to mock-treated samples for OVCAR5-RFP and ovc316 (Figure 5(c), S6). A similar kinetics was seen when DSG2 was measured in the culture supernatant by ELISA (Figure 5(d)). This plot also shows that ovc316 cells shed DSG2 to some extent even without cisplatin treatment.

### Discussion

While over 80% of advanced-stage ovarian epithelial cancer patients attain clinical remission with standard platinum/paclitaxel-based chemotherapy, the vast majority of them will relapse within two to 5 y.<sup>39,40</sup> It has become a standard clinical practice to include CA125 testing in patient surveillance. Elevation in CA125 often precedes clinical evidence of relapse by imaging or physical exam.<sup>41</sup> Data from a large randomized clinical trial, however, demonstrate no survival advantage from CA125 screening.<sup>42</sup> HE4 can predict ovarian cancer recurrence earlier than CA125 and it can be elevated in patients that do not express CA125 at sufficient levels to make a clinical decision.<sup>36</sup>

Our findings that DSG2 is upregulated in ovarian cancer are in line with reports on other cancers. Proteomics analysis of ascites from ovarian cancer patients identified DSG2 as one of the top hits of upregulated proteins.<sup>25</sup> Moreover, the survival of HCC patients with high DSG2 mRNA and protein expression was shorter.<sup>16</sup> However, there are studies with melanoma, pancreatic, and colon cancer cell lines and xenograft tumor models indicating enhanced metastasis and aggressiveness upon suppression or loss of DSG2 expression.<sup>16,43,44</sup> Furthermore, low DSG2 expression has been associated with poor clinical outcomes in certain types of cancer such as prostate<sup>45</sup> and gastric<sup>46</sup> cancers. This was explained by the

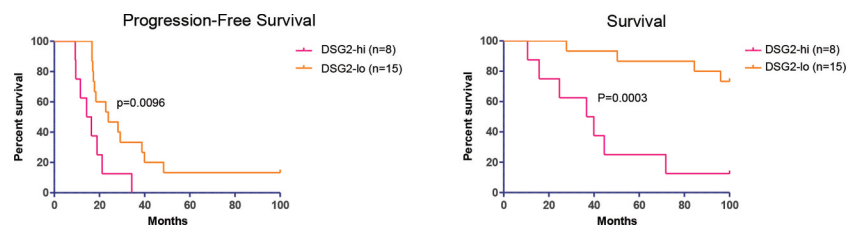


**Figure 4.** DSG2 expression correlates with ovarian cancer progression-free survival (PFS) and general survival. A cohort of ovarian cancer patients from the Fred Hutchinson Cancer Center were placed into DSG-high or DSG-low expressing groups as defined by a threshold mean serum DSG2 concentration of 828 ng/mL. Analyses were done for months of PFS and general survival, using the Log-Rank (Mantel-Cox) tests for comparisons between populations.  $P$  values are results of the Log-Rank test for comparison of survival between populations.

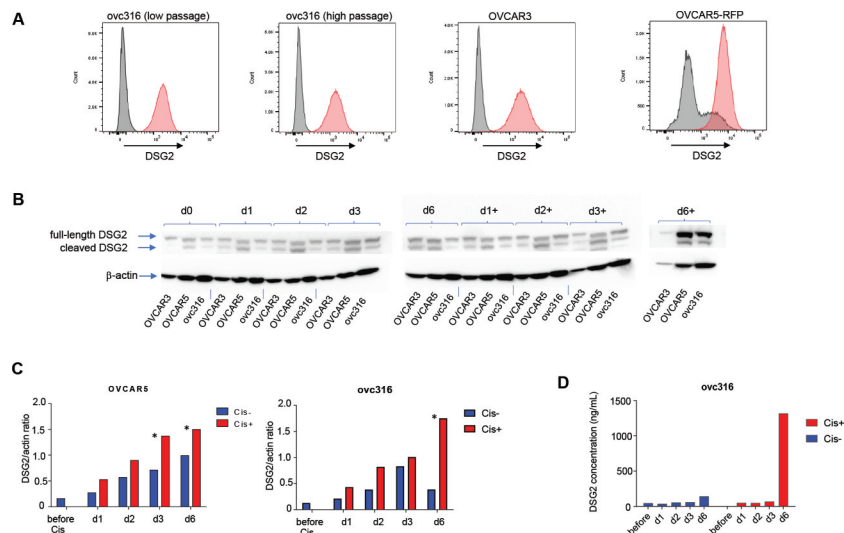


**Figure 5.** DSG2 expression in ovarian cancer cell lines is upregulated in response to cisplatin. **(A)** Ovc316 (passage 4 and 15 after isolation from tumors), OVCAR3, and OVCAR5-RFP cell cultures were analyzed for DSG2 expression by flow cytometry, indicated by the red curve. **(B)** Ovc316 (passage 4), OVCAR3, and OVCAR5-RFP cells were cultured with or without cisplatin added to the medium, at a concentration of 2.5  $\mu$ M. Cells were harvested before adding cisplatin ("day 0") and at days 1, 2, 3, and 6 (+ indicating cisplatin-treated cells). Cell lysates were analyzed by Western Blot. Bands specific to DSG2 and  $\beta$ -actin are indicated. **(C)** DSG2/actin ratios as quantified by ImageJ are shown. The study was done in triplicates. The standard deviation was less than 5%. \*:  $p < .05$ . **(D)** DSG2 shed in serum as quantified by ELISA is shown for the ovc316 cell line at days 1, 2, 3, 6 with and without cisplatin treatment.

observation that loss of epithelial junctions and downregulation of epithelial proteins such as DSG2 is associated with epithelial-to-mesenchymal transition (EMT), a central mechanism for cancer cell mobility and metastasis.<sup>47</sup> However, this assumption does not consider that following invasion or metastasis, cells that have undergone the process of EMT can also revert to a well-differentiated epithelial phenotype.<sup>48</sup> In support, there exist numerous examples of advanced carcinomas showing that mesenchymal cells can regain characteristics of epithelial cells or undergo

mesenchymal to epithelial transition (MET).<sup>48</sup> In an attempt to demonstrate that gaining epithelial features, specifically an increase in DSG2 expression, can increase tumor progression, we used a pair of syngeneic cell lines derived from the histiocytic lymphoma cell line U937 described previously.<sup>7</sup> U937-DSG2 cells stably expressed DSG2 after lentivirus vector transduction, while U937 was negative for DSG2 (see Figure 3(b) in reference<sup>7</sup>). Figure 6 shows that after subcutaneous injection into immunodeficient mice, tumors derived from U937-DSG2 grew significantly faster than U937 tumors.

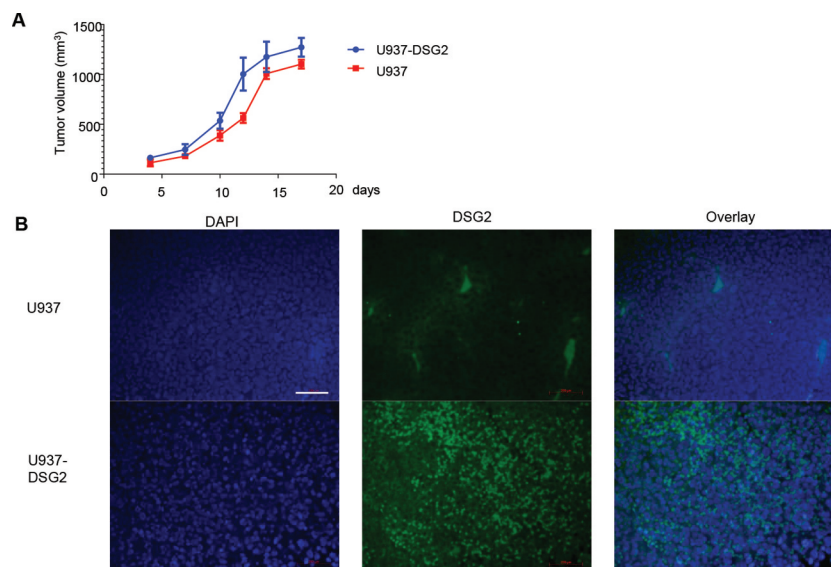


**Figure 6.** Growth of xenograft tumors derived from injected DSG2 negative U937 cells and U937-DSG2 cells that ectopically express DSG2 after lentivirus gene transfer. CB17 mice were implanted with U937 cell xenografts expressing DSG2 or not expressing DSG2. Tumors were allowed to grow until 1000  $\text{mm}^3$  before sacrifice. **(A)** Growth curves of mice,  $N = 5$ . The difference between the groups is significant ( $p < .01$ ) (two-way ANOVA). **(B)** Tumor sections were taken after fixation in formaldehyde and stained with DAPI (blue) for nuclei and DSG2 (green). Overlays are shown on the right. The scale bar is 200  $\mu$ m.

Our study indicates that DSG2 can be used as a potential biomarker for ovarian cancer that correlates with the grade, chemoresistance, progression-free survival, and general survival. The observation of progressively higher DSG2 expression with higher cancer grade classification was notable, although the differences between grades 2 and 3 did not reach statistical significance, as the difference in PFS and general survival between DSG2-low and DSG2-high expressing populations, seen in two separate cohorts which lend further credence to the use of DSG2 expression levels as a prognostic indicator for ovarian cancer patients' survival. This strong correlation is not supported by a recent study that analyzed DSG2 signals on serous ovarian cancer sections and DSG2 mRNA levels in correlation with survival and clinicopathological data.<sup>27</sup> Potential reasons for this could be the use of different techniques for measuring DSG2.

Our *in vitro* studies with ovarian cancer cell lines indicate that DSG2 is upregulated in response to cisplatin treatment, which may represent an autocatalytic mechanism to initiate or enhance chemo-resistance. More studies with primary ovarian cancer cell lines and animal models, including human-DSG2 transgenic mice with syngeneic tumors,<sup>10,49</sup> need to be done to understand the mechanism behind DSG2 upregulation by cisplatin. Considering the higher mutation rate and genomic instability higher in high-grade serous ovarian cancer, it is possible that chemotherapy selects for tumor cell clones with higher DSG2 expression.<sup>50</sup> On the other hand, gene alteration and copy number analysis of DSG2 (Fig.S7) did not reveal a large mutational burden on DSG2 in ovarian cancer cases (alterations in 6.86% of cases), and copy number alterations did not deviate significantly according to the z-scores. This seems to indicate that DSG2 mutations or alterations in the genome do not play a significant role in driving ovarian cancer cases.

While our finding might help to better understand mechanistic aspects of chemoresistance, they have direct practical implication for our upcoming clinical trial with our recombinant junction opener JO in combination with Doxil® in patients with progressive, persistent, or recurrent ovarian/fallopian tube cancer, who have previously received standard therapies. DSG2 as a tumor marker and target also holds implications for oncolytic adenovirus therapy, and indeed Ad5/3 oncolytic viruses show increased efficacy on ovarian cancer cells with increased DSG2 RNA expression.<sup>51</sup> This study also included retrospective analyses of phase I clinical trial of an Ad5/3-based oncolytic adenovirus (ONCOS-102) in 12 patients with varied tumors indicated a correlation between viral genomes in blood and DSG2 RNA expression.

To better understand the potential for clinical translation, our study requires further research. Considering cancer heterogeneity, larger patient cohorts are needed to consolidate the correlation between serum DSG2 concentrations and survival of ovarian cancer patients. Furthermore, longitudinal DSG2 measurements during and after chemotherapy could provide valuable information. The influence of soluble DSG2 in blood and potential sequestration of DSG2-targeting recombinant junction openers and oncolytic viruses has to be studied. Some of this work can be done in the DSG2-transgenic mouse tumor model.<sup>49</sup>

Also, the role of other members of the desmoglein (DSG1 and DSG3) and desmocollin (DSC1-3) families in cancer progression warrants further analysis. Notably, in pancreatic cancer patients, high DSG3 expression was associated with poor overall survival.<sup>52</sup> Our initial attempt, using publicly available databases, including the TCGA, did not find a significant association between DSG1, DSG3, and DSC1-3 expression and chemoresistance or ovarian cancer progression and death (Fig.S8).

Based on the data reported here we suggest that DSG2 may be useful in stratifying ovarian cancer patients, predicting chemoresistance, and as a companion diagnostic for treatments targeting DSG2.

## Materials and methods

### Cells

Ovc316 cells are primary ovarian cancer cells derived from a patient biopsy, specifically one of the high-grade serous ovarian cancer.<sup>34</sup> The authors had no access to data that would identify the patient(s). Work with patient-derived tumor cells and biopsies was approved by the Fred Hutchinson Cancer Research Center Institutional Review Board (protocol: 6289 "Secondary use of human cells"). Ovc316, OVCAR3 (ATCC: HTB-161), and OVCAR5-RFP (Cell Biolabs: AKR-254) were cultured in MEGM (MEBM containing 3 µg/L hEGF, 5 µg/L insulin, 5 mg/L hydrocortisone, 26 mg/L bovine pituitary extract, 25 mg/L amphotericin B) (Lonza), supplemented with 10% FBS (Gibco), 100 IU penicillin, 100 mg/L streptomycin. Xenograft tumors were established by injection of  $2 \times 10^6$  ovc316 cells (1:1 with Matrigel) into the mammary fat pad on immunodeficient CB17 mice. U937 (ATCC CRL-1593.2) and U937-DSG2 cells were described previously.<sup>7</sup>

### Xenograft tumor studies

These studies were carried out in strict accordance with the recommendations in the Guide for the Care and Use of Laboratory Animals of the National Institutes of Health. The protocol was approved by the Institutional Animal Care and Use Committee of the University of Washington, Seattle, WA (Protocol: 3108-01). Mice were housed in specific-pathogen-free facilities. Immunodeficient NOD.CB17-Prkdcscid/J (CB17) mice were obtained from the Jackson Laboratory. Xenograft tumors were established by injection of  $2 \times 10^6$  ovc316, U937, or U937-DSG2 cells (mixed 1:1 with Matrigel) into the mammary fat pad of mice. Tumor volumes were measured as described previously.<sup>53</sup>

### Immunohistochemistry staining for DSG2

Paraffin sections of ovarian biopsies as well as frozen cancer samples were obtained from the Translational Outcomes Research (TOR) Repository, Fred Hutchinson Cancer Research Center. The ovarian tissue array was obtained from Biomax Inc (Part Number OV208a) (Rockville). The array contains 207 core sections from 69 cases as well as information

on TNM, clinical stage, and pathology grade as classified according to WHO 1999 Classifications by a certified pathologist. Slides were deparaffinized and hydrated through immersion in xylene, decreasing concentrations of ethanol (100%-95%-80%-70%), and water. Slides were then immersed in 0.3% hydrogen peroxide, followed by an additional rinse of water to eliminate endogenous peroxidase. Slides were then placed in 1% Unmasking solution (Vector Labs) and placed in a miniature autoclave (at up to 125°C for 1 h) for antigen retrieval. Slides were incubated in 2.5% normal horse serum (NHS) blocking solution (Vector Labs) for 20 minutes at room temperature, followed by incubation with the primary antibody, goat anti-human DSG2 (Abcam) (diluted 1:200 in PBS/1% NHS) overnight at 4°C. A goat IgG isotype control from Novus Biologicals (NB410-28088) was used. Following an additional wash in PBS, 4 drops of ImmPRESS Reagent Kit anti-goat Ig (Vector Labs) were added, and slides were incubated for 30 min. After washing, 2 drops of Polink-2 HRP Kit with DAB Chromogen (Golden Bridge International, Inc) were added and allowed to develop for around 5 minutes before washing with water. Sections were counterstained with Mayer's Hematoxylin (Sigma-Aldrich, St. Louis, MO) for 5 to 10 seconds and washed with water. After the slides dried, 3–5 drops of VectaMount (Vector Labs) were added to the slide with a coverslip placed on top. Images were taken with a Leica DMLB microscope (Wetzlar), using Leica DFC300 FX Digital camera and Leica Application Suite Version 2.4.1 R1 software.

For quantitation, tissue microarray slides were scanned in brightfield with a 20× objective using a NanoZoomer Digital Pathology System (Hamamatsu City). The digital image was then imported into Visiopharm software (Hoersholm, Denmark) for analysis. Using the Visiopharm Image Analysis module, regions of interests (ROI) were manually drawn around each tissue core. By converting the initial digital image into grayscale values using two features, RGB – B and RGB – R, the Visiopharm software was trained to label positive staining, DSG2, and background tissue counterstain, hematoxylin, using a project-specific configuration based on a threshold of pixel values based on the difference in intensity between normal tissue and cancerous tissue. ROIs were manually designated to exclude non-epithelial tissue. The ROIs were processed in batch mode using this configuration to generate the desired per area outputs and analyzed at 100%.

### **DSG2 immunofluorescence staining on sections of ovc316 xenograft tumors**

Cryosections of xenograft tumors were fixed in 4% paraformaldehyde for 15 minutes at room temperature then rinsed with PBS three times. The slide was then placed in a blocking buffer (2% nonfat milk in PBS) for 60 minutes at room temperature. Primary antibodies mouse anti-DSG2 (6D8, Abcam) and rabbit anti-Claudin7 (ab27487, Abcam, UK) were prepared at a 1:50 dilution. Blocking solution was removed and slides were incubated with primary antibody overnight at 4°C. After washing, slides were incubated with the secondary antibody mix (FITC-goat-anti-mouse Ab, PE-goat-anti-rabbit Ab) for 1 h at room temperature in the dark. Slides were washed with PBS before mounting with Vectashield Antifade

Mounting Medium + DAPI (Vector Labs) and were viewed under a Leica microscope as described above.

### **Western blot**

Mini-PROTEAN precast gels (BIO-RAD) with 4–15% gradient polyacrylamide were used. A total of 1 µg protein diluted 1:1 in 2 × loading buffer (10 mM Tris-HCl, pH = 6.8, 200 mM DTT, 4% SDS, 20% glycerol, 0.2% bromophenol blue) was loaded per lane. Samples were boiled for 5 min. The following running buffer was used: 25 mM Tris, pH = 8.3, 0.192 M glycine, 0.1% SDS. After electrophoresis, proteins were transferred to nitrocellulose and incubated with the anti-DSG2 antibody 6D8 as described previously and a secondary anti-mouse IgG HRP conjugate.<sup>7</sup> Selected Western blots were scanned and quantified using the ImageJ 1.32 software (National Institutes of Health).

### **DSG2 ELISA**

The ELISA was performed using a rabbit polyclonal anti-human desmoglein-2 antibody (R&D System, Catalog # AF947) as a capture antibody at a concentration of 2 µg/ml in 0.1 M Na-carbonate, pH = 9.6 buffer. Plates were washed with TBS-T (Tris-buffered saline + 0.05% Tween-20) before blocking with Starting Block<sup>TM</sup> (PBS) Blocking Buffer (Thermo Scientific, Prod #37538). Human serum samples were analyzed in three dilutions (1:10, 1:50, and 1:100) using Blocking Buffer as a dilutant. For detection, the mouse monoclonal antibody 6D8 directed against ECD3 (AbD Serotec) was used at a 1:100 dilution. After three washes, goat anti-mouse IgG-HRP peroxidase (BD Pharmingen) was added at a 1:1000 dilution in blocking buffer. 1-Step<sup>TM</sup> Ultra TMB-ELISA (Thermo Scientific) was used as a substrate. Recombinant human-DSG2 protein used for the standard curve was from Leinco Technologies, Inc. The detection limit of the DSG2 ELISA was 0.5 ng/ml.

### **mRNA quantification**

Clinical biopsy samples from ovarian cancer patients were used for RNAseq. RNA was extracted from samples using RNeasy Plus Mini or AllPrep RNA/DNA kits (QIAGEN). The quality of the RNA was assessed on an Agilent 2100 Bioanalyzer. Samples with RNA integrity number (RIN) greater than 7 were diluted to 50 ng/mL for sequencing library preparation using TruSeq Sample Preparation Kit (Illumina). Starting with approximately 1 µg of total RNA, mRNA was isolated with oligo-dT capture beads, and then fragmented and converted to cDNA with random hexamer-primed reverse transcription and second-strand synthesis. Resulting cDNAs were fragmented by sonication and size-selected for molecules of ~300 bp. Ligation of barcoded sequencing adapters was then performed according to the manufacturer's recommendations. The cDNA samples underwent multiplex sequencing, with one to four samples per lane, on the Illumina HiSeq 2000 to yield 50 bp paired-end sequences. This process yielded between 54.6 M and 367.0 M sequences passing the default Illumina quality control filters. RNA-seq data analysis was performed as described elsewhere.<sup>54</sup>

## TCGA data mining

Data regarding the exome DSG2 mutational profiling of ovarian cancer cases were analyzed and visualized using cBioPortal (Memorial Sloan-Kettering Center). The TCGA-FirehoseLegacy-OV data set was used. Visualizations for genome alteration frequency and the copy number alterations were generated using putative numbers from GISTIC and mRNA expression z-Scores.

## Clinical samples and statistical analyses

Ovarian cancer biopsies and sections were provided by the Pacific Ovarian Cancer Research Consortium (POCRC) Specimen Repository without any confidential information which would serve to identify a patient (Fred Hutchinson Cancer Research Center, IRB protocol # 6289). Statistical analyses were carried out using Graphpad Prism (San Diego, CA, USA).

## Acknowledgments

The authors would like to thank Lindsay Bergan and Sarah Hawley (TOR, FHCR) for providing cancer samples and sections. We are grateful to the UW Histology and Imaging Core (Brian Johnson and Sarah Lindhartsen) for assistance with digital image quantification and analysis. Furthermore, we thank Marty McIntosh and Michèl Schummer (FHCR) for access to their databases. This work was supported by DoD grant OC160162 (AL), Andy Hill CARE grant BRK 201801-02 (AL), 2R44CA206607-02A1 (DC).

## Author contributions

A.L. designed the experiments. J.H. P.B., H.W. A.Q., C.C. performed the experiments. C.D. and D.C. provided critical material and comments on the manuscript. J.K. and A.L. wrote the manuscript.

## Additional information:

This work was supported by DoD grant OC160162 (AL), Andy Hill CARE grant BRK 201801-02 (AL), 2R44CA206607-02A1 (DC).

## References

- Key Statistics for Ovarian Cancer. Available from URL: <https://www.cancer.org/cancer/ovarian-cancer/about/key-statistics.html>
- Curti BD. Physical barriers to drug delivery in tumors. *Crit Rev Oncol Hematol.* 1993;14:29–39. doi:10.1016/1040-8428(93)90004-N.
- Anderson JM. Molecular structure of tight junctions and their role in epithelial transport. *Physiology.* 2001;16:126–130. doi:10.1152/physiologyonline.2001.16.3.126.
- Anderson JM, Van Itallie CM. Physiology and function of the tight junction. *Cold Spring Harb Perspect Biol.* 2009;1:a002584. doi:10.1101/cshperspect.a002584.
- Guttman JA, Finlay BB. Tight junctions as targets of infectious agents. *Biochimica Et Biophysica Acta (Bba)-biomembranes.* 2009;1788:832–841. doi:10.1016/j.bbame.2008.10.028.
- Bergelson JM, Cunningham JA, Droguett G, Kurt-Jones EA, Krithivas A, Hong JS, Horwitz MS, Crowell RL, Finberg RW. Isolation of a common receptor for Coxsackie B viruses and adenoviruses 2 and 5. *Science.* 1997;275:1320–1323. doi:10.1126/science.275.5304.1320.
- Wang H, Li ZY, Liu Y, Persson J, Beyer I, Moller T, Koyuncu D, Drescher MR, Strauss R, Zhang XB, et al. Desmoglein 2 is a receptor for adenovirus serotypes 3, 7, 11 and 14. *Nat Med.* 2011;17:96–104. doi:10.1038/nm.2270.
- Garrod D, Chidgey M. Desmosome structure, composition and function. *Biochimica Et Biophysica Acta (Bba)-biomembranes.* 2008;1778:572–587. doi:10.1016/j.bbame.2007.07.014.
- Klessner JL, Desai BV, Amargo EV, Getsios S, Green KJ, Nusrat A. EGFR and ADAMs cooperate to regulate shedding and endocytic trafficking of the desmosomal cadherin desmoglein 2. *Mol Biol Cell.* 2009;20:328–337. doi:10.1091/mbc.e08-04-0356.
- Wang H, Ducournau C, Saydaminova K, Richter M, Yumul R, Ho M, Carter D, Zubieta C, Fender P, Lieber A. Intracellular signaling and desmoglein 2 shedding triggered by human adenoviruses Ad3, Ad14, and Ad14P1. *J Virol.* 2015;89:10841–10859. doi:10.1128/JVI.01425-15.
- Brennan D, Mahoney MG. Increased expression of Dsg2 in malignant skin carcinomas: A tissue-microarray based study. *Cell Adh Migr.* 2009;3:148–154. doi:10.4161/cam.3.2.7539.
- Harada H, Iwatsuki K, Ohtsuka M, Han GW, Kaneko F. Abnormal desmoglein expression by squamous cell carcinoma cells. *Acta Derm Venereol.* 1996;76:417–420.
- Cai F, Zhu Q, Miao Y, Shen S, Su X, Shi Y. Desmoglein-2 is overexpressed in non-small cell lung cancer tissues and its knockdown suppresses NSCLC growth by regulation of p27 and CDK2. *J Cancer Res Clin Oncol.* 2017;143:59–69. doi:10.1007/s00432-016-2250-0.
- Sun R, Ma C, Wang W, Yang S. Upregulation of desmoglein 2 and its clinical value in lung adenocarcinoma: a comprehensive analysis by multiple bioinformatics methods. *PeerJ.* 2020;8:e8420. doi:10.7717/peerj.8420.
- Jin R, Wang X, Zang R, Liu C, Zheng S, Li H, Sun N, He J. Desmoglein-2 modulates tumor progression and osimertinib drug resistance through the EGFR/Src/PAK1 pathway in lung adenocarcinoma. *Cancer Lett.* 2020;483:46–58. doi:10.1016/j.canlet.2020.04.001.
- Han CP, Yu YH, Wang AG, Tian Y, Zhang HT, Zheng ZM, Liu YS. Desmoglein-2 overexpression predicts poor prognosis in hepatocellular carcinoma patients. *Eur Rev Med Pharmacol Sci.* 2018;22:5481–5489.
- Biedermann K, Vogelsang H, Becker I, Plaschke S, Siewert JR, Hofler H, Keller G. Desmoglein 2 is expressed abnormally rather than mutated in familial and sporadic gastric cancer. *J Pathol.* 2005;207:199–206. doi:10.1002/path.1821.
- Grantab R, Sivananthan S, Tannock IF. The penetration of anticancer drugs through tumor tissue as a function of cellular adhesion and packing density of tumor cells. *Cancer Res.* 2006;66:1033–1039. doi:10.1158/0008-5472.CAN-05-3077.
- Strauss R, Sova P, Liu Y, Li Z-Y, Tuve S, Pritchard D, Brinkkoetter P, Moller T, Wildner O, Pesonen S, et al. Epithelial phenotype of ovarian cancer mediates resistance to oncolytic adenoviruses. *Cancer Res.* 2009;15:5115–5125. doi:10.1158/0008-5472.CAN-09-0645.
- Beyer I, Cao H, Persson J, Song H, Richter M, Feng Q, Yumul R, van Rensburg R, Li Z, Berenson R, et al. Coadministration of epithelial junction opener JO-1 improves the efficacy and safety of chemotherapeutic drugs. *Clin Cancer Res.* 2012;18:3340–3351. doi:10.1158/1078-0432.CCR-11-3213.
- Beyer I, van Rensburg R, Lieber A. Overcoming physical barriers in cancer therapy. *Tissue Barriers.* 2013;1:e23647. doi:10.4161/tisb.23647.
- Beyer I, van Rensburg R, Strauss R, Li Z, Wang H, Persson J, Yumul R, Feng Q, Song H, Bartek J, et al. Epithelial junction opener JO-1 improves monoclonal antibody therapy of cancer. *Cancer Res.* 2011;71:7080–7090. doi:10.1158/0008-5472.CAN-11-2009.
- Wang CE, Yumul RC, Lin J, Cheng Y, Lieber A, Pun SH. Junction opener protein increases nanoparticle accumulation in solid tumors. *J Control Release.* 2018;272:9–16. doi:10.1016/j.jconrel.2017.12.032.
- Wang H, Li Z, Yumul R, Lara S, Hemminki A, Fender P, Lieber A. Multimerization of adenovirus serotype 3 fiber knob domains is

- required for efficient binding of virus to desmoglein 2 and subsequent opening of epithelial junctions. *J Virol.* 2011;85:6390–6402. doi:10.1128/JVI.00514-11.
25. Kuk C, Kulasingham V, Gunawardana CG, Smith CR, Batruch I, Diamandis EP. Mining the ovarian cancer ascites proteome for potential ovarian cancer biomarkers. *Mol Cell Proteomics.* 2009;8:661–669. doi:10.1074/mcp.M800313-MCP200.
  26. Xie H, Xu H, Hou Y, Cai Y, Rong Z, Song W, Wang W, Li K. Integrative prognostic subtype discovery in high-grade serous ovarian cancer. *J Cell Biochem.* 2019;120:18659–18666. doi:10.1002/jcb.29049.
  27. Chen L, Liu X, Zhang J, Liu Y, Gao A, Xu Y, Lin Y, Du Q, Zhu Z, Hu Y, et al. Characterization of desmoglein 2 expression in ovarian serous tumors and its prognostic significance in high-grade serous carcinoma. *Int J Clin Exp Pathol.* 2018;11:4977–4986.
  28. Richter M, Yumul R, Wang H, Saydaminova K, Ho M, May D, Baldessari A, Gough M, Drescher C, Urban N, et al. Preclinical safety and efficacy studies with an affinity-enhanced epithelial junction opener and PEGylated liposomal doxorubicin. *Mol Ther Methods Clin Dev.* 2015;2:15005. doi:10.1038/mtm.2015.5.
  29. Kim KH, Dmitriev IP, Saddekni S, Kashentseva EA, Harris RD, Aurigemma R, Bae S, Singh KP, Siegal GP, Curiel DT, et al. A phase I clinical trial of Ad5/3-Delta24, a novel serotype-chimeric, infectivity-enhanced, conditionally-replicative adenovirus (CRAd), in patients with recurrent ovarian cancer. *Gynecol Oncol.* 2013;130:518–524. doi:10.1016/j.ygyno.2013.06.003.
  30. Hemminki O, Bauerschmitz G, Hemmi S, Kanerva A, Cerullo V, Pesonen S, Hemminki A. Preclinical and clinical data with a fully serotype 3 oncolytic adenovirus Ad3-hTERT-E1A in the treatment of advanced solid tumors. *Molecular Therapy.* 2010;18:S74.
  31. Koski A, Kangasniemi L, Escutenaire S, Pesonen S, Cerullo V, Diaconu I, Nokisalmi P, Raki M, Rajacki M, Guse K, et al. Treatment of cancer patients with a serotype 5/3 chimeric oncolytic adenovirus expressing GMCSF. *Mol Ther.* 2010;18:1874–1884. doi:10.1038/mt.2010.161.
  32. Kuryk L, Møller ASW. Chimeric oncolytic Ad5/3 virus replicates and lyses ovarian cancer cells through desmoglein-2 cell entry receptor. *J Med Virol.* 2020;92(9):1309–1315.
  33. Saydaminova K, Strauss R, Xie M, Bartek J, Richter M, van Rensburg R, Drescher C, Ehrhardt A, Ding S, Lieber A. Sensitizing ovarian cancer cells to chemotherapy by interfering with pathways that are involved in the formation of cancer stem cells. *Cancer Biol Ther.* 2016;17:1079–1088. doi:10.1080/15384047.2016.1219819.
  34. Strauss R, Li ZY, Liu Y, Beyer I, Persson J, Sova P, Moller T, Pesonen S, Hemminki A, Hamerlik P, et al. Analysis of epithelial and mesenchymal markers in ovarian cancer reveals phenotypic heterogeneity and plasticity. *PLoS One.* 2011;6:e16186. doi:10.1371/journal.pone.0016186.
  35. Rustin GJ, Vergote I, Eisenhauer E, Pujade-Lauraine E, Quinn M, Thigpen T, Du Bois A, Kristensen G, Jakobsen A, Sagae S, et al. Definitions for response and progression in ovarian cancer clinical trials incorporating RECIST 1.1 and CA 125 agreed by the gynecological cancer intergroup (GCIg). *Int J Gynecol Cancer.* 2011;21:419–423. doi:10.1097/IGC.0b013e3182070f17.
  36. Schummer M, Drescher C, Forrest R, Gough S, Thorpe J, Hellstrom I, Hellstrom KE, Urban N. Evaluation of ovarian cancer remission markers HE4, MMP7 and Mesothelin by comparison to the established marker CA125. *Gynecol Oncol.* 2012;125:65–69. doi:10.1016/j.ygyno.2011.11.050.
  37. Tannock IF, Lee CM, Tunggal JK, Cowan DS, Egorin MJ. Limited penetration of anticancer drugs through tumor tissue: a potential cause of resistance of solid tumors to chemotherapy. *Clin Cancer Res.* 2002;8:878–884.
  38. Minchinton AI, Tannock IF. Drug penetration in solid tumours. *Nat Rev Cancer.* 2006;6:583–592. doi:10.1038/nrc1893.
  39. Ozols RF, Bundy BN, Greer BE, Fowler JM, Clarke-Pearson D, Burger RA, Mannel RS, DeGeest K, Hartenbach EM, Baergen R, et al. Phase III trial of carboplatin and paclitaxel compared with cisplatin and paclitaxel in patients with optimally resected stage III ovarian cancer: a gynecologic oncology group study. *J Clin Oncol.* 2003;21:3194–3200. doi:10.1200/JCO.2003.02.153.
  40. Cannistra SA. Cancer of the ovary. *N Engl J Med.* 2004;351:2519–2529. doi:10.1056/NEJMra041842.
  41. Rustin GJ, Nelstrop AE, Tuxen MK, Lambert HE. Defining progression of ovarian carcinoma during follow-up according to CA 125: a north Thames ovary group study. *Ann Oncol.* 1996;7:361–364. doi:10.1093/oxfordjournals.annonc.a010602.
  42. Rustin GJ, van der Burg ME, Griffin CL, Guthrie D, Lamont A, Jayson GC, Kristensen G, Mediola C, Coens C, Qian W, et al. Early versus delayed treatment of relapsed ovarian cancer (MRC OV05/EORTC 55955): a randomised trial. *Lancet.* 2010;376:1155–1163. doi:10.1016/S0140-6736(10)61268-8.
  43. Peitsch WK, Doerflinger Y, Fischer-Colbrie R, Huck V, Bauer AT, Utikal J, Goerdts S, Schneider SW. Desmoglein 2 depletion leads to increased migration and upregulation of the chemoattractant secretoneurin in melanoma cells. *PLoS One.* 2014;9:e89491. doi:10.1371/journal.pone.0089491.
  44. Kamekura R, Kolegraff KN, Nava P, Hilgarth RS, Feng M, Parkos CA, Nusrat A. Loss of the desmosomal cadherin desmoglein-2 suppresses colon cancer cell proliferation through EGFR signaling. *Oncogene.* 2014;33:4531–4536. doi:10.1038/onc.2013.442.
  45. Barber AG, Castillo-Martin M, Bonal DM, Rybicki BA, Christiano AM, Cordon-Cardo C, Robson CN. Characterization of desmoglein expression in the normal prostatic gland. Desmoglein 2 is an independent prognostic factor for aggressive prostate cancer. *PLoS One.* 2014;9:e98786. doi:10.1371/journal.pone.0098786.
  46. Yashiro M, Nishioka N, Hirakawa K. Decreased expression of the adhesion molecule desmoglein-2 is associated with diffuse-type gastric carcinoma. *Eur J Cancer.* 2006;42:2397–2403. doi:10.1016/j.ejca.2006.03.024.
  47. Hutz K, Zeiler J, Sachs L, Ormanns S, Spindler V. Loss of desmoglein 2 promotes tumorigenic behavior in pancreatic cancer cells. *Mol Carcinog.* 2017;56:1884–1895. doi:10.1002/mc.22644.
  48. Christiansen JJ, Rajasekaran AK. Reassessing epithelial to mesenchymal transition as a prerequisite for carcinoma invasion and metastasis. *Cancer Res.* 2006;66:8319–8326. doi:10.1158/0008-5472.CAN-06-0410.
  49. Wang H, Beyer I, Persson J, Song H, Li Z, Richter M, Cao H, van Rensburg R, Yao X, Hudkins K, et al. A new human DSG2-transgenic mouse model for studying the tropism and pathology of human adenoviruses. *J Virol.* 2012;86:6286–6302.
  50. Seiden MV. Progress in gynecologic cancer. *Semin Oncol.* 2009;36:90. doi:10.1053/j.seminoncol.2008.12.010.
  51. Kuryk L, Moller AW. Chimeric oncolytic Ad5/3 virus replicates and lyses ovarian cancer cells through desmoglein-2 cell entry receptor. *J Med Virol.* 2020;92:1309–1315. doi:10.1002/jmv.25677.
  52. Ormanns S, Altendorf-Hofmann A, Jackstadt R, Horst D, Assmann G, Zhao Y, Bruns C, Kirchner T, Knosel T. Desmogleins as prognostic biomarkers in resected pancreatic ductal adenocarcinoma. *Br J Cancer.* 2015;113:1460–1466. doi:10.1038/bjc.2015.362.
  53. Yumul R, Richter M, Lu ZZ, Saydaminova K, Wang H, Wang CH, Carter D, Lieber A. Epithelial junction opener improves oncolytic adenovirus therapy in mouse tumor models. *Hum Gene Ther.* 2016;27:325–337. doi:10.1089/hum.2016.022.
  54. Chou J, Fitzgibbon MP, Mortales CL, Towlerton AM, Upton MP, Yeung RS, McIntosh MW, Warren EH, Cheung ST. Phenotypic and transcriptional fidelity of patient-derived colon cancer xenografts in immune-deficient mice. *PLoS One.* 2013;8:e79874. doi:10.1371/journal.pone.0079874.